Performance Evaluation of PLL Algorithms for Single-phase Grid-connected Systems

Sidelmo M. Silva sidelmo@ieee.org
Bruno M. Lopes bmarcianol@yahoo.com.br
Braz J. Cardoso Filho cardosob@cpdee.ufmg.br
Rodrigo P. Campana rpcampana@yahoo.com.br
Wallace C. Boaventura wventura@cpdee.ufmg.br

Universidade Federal de Minas Gerais
Depto. de Engenharia Elétrica
Av. Antônio Carlos, 6627 – Pampulha
31270-010 – Belo Horizonte – MG – Brazil

***Abstract* – Phase angle, frequency and amplitude of the utility voltage vector are basic information for an increasing number of grid-connected power conditioning equipments, such as PWM rectifiers, uninterruptible power systems (UPS), voltage sag compensators and the emerging distributed generation systems. For these applications, accurate tracking of the utility voltage vector is essential to ensure correct operation of the control system. This paper presents a comparative study of synchronous reference frame PLL algorithms for single-phase systems. Simulation and experimental results, including operation of the PLL structures under distorted utility conditions are presented, to allow a performance evaluation of the PLL algorithms.**

Keywords – Phase-locked loop, grid-connected system, distorted utility conditions.

I. INTRODUCTION

Phase angle, frequency and amplitude of the utility voltage vector are basic information for an increasing number of grid-connected power conditioning equipments, such as Pulse Width Modulation (PWM) rectifiers, uninterruptible power systems (UPS), voltage sag compensators and the emerging distributed generation systems. For these applications, accurate tracking of the utility voltage vector is essential to ensure correct operation of the control system.

Recently, there has been an increasing interest in PLL topologies for grid-connected systems [1-5]. The three-phase PLL discussed in [4] uses a synchronous reference frame (SRF) to detect phase angle, frequency and amplitude of the three-phase voltages of the utility system. For single-phase systems, similar approaches can be utilized, as presented in [1-3]. In [1-2], the quadrature voltage, required for a SRF PLL, is generated from a single-phase input, through the use of an inverse Park transformation. In [3], the quadrature signal is generated by using the Hilbert transformer. A simpler way of generating the quadrature signal is through the use of a transport delay block, which is responsible for introducing a phase shift of *90* degrees with respect to the fundamental frequency of the input signal.

This paper presents a comparative study of SRF PLL algorithms for single-phase grid-connected systems, including an evaluation of their behavior under distorted utility conditions. Simulation and experimental results with distorted utility conditions are used to illustrate the operation of the PLL structures.

II. PLL STRUCTURES CONSIDERED

Inverse Park-Based PLL

Figure 1 shows a schematic diagram of the single-phase PLL structure, introduced in [1-2]. As it can be seen, a single-phase voltage (V_β) and an internally generated signal (V_α) are used as inputs to a Park transformation block ($\alpha\beta$-dq). The d-axis output of the Park transformation is used in a control loop to obtain phase and frequency information of the input signal. V_α is obtained through the use of an inverse Park transformation, where the inputs are the d and q-axis outputs of the Park transformation (dq-$\alpha\beta$). fed through first-order pole blocks. The poles are used to introduce an energy storage element in the internal feedback loops.

Figure 2 shows the reference frames considered in the transformations. Eq. (1) and (2) show the direct and inverse Park transformation utilized.

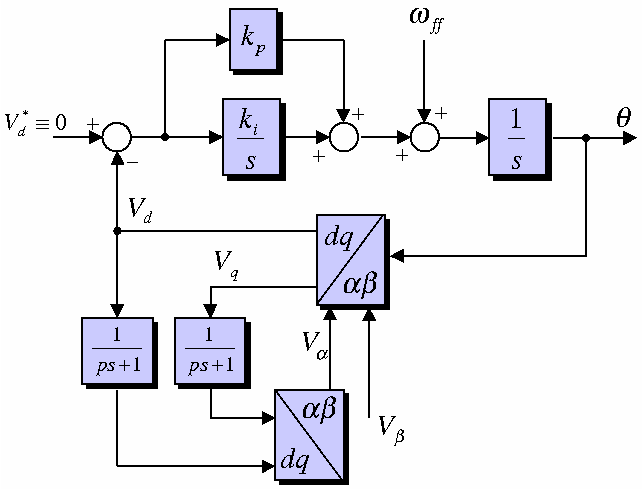

Figure 1 – Single-phase PLL algorithm based on a inverse Park transformation for the generation of the quadrature signal.

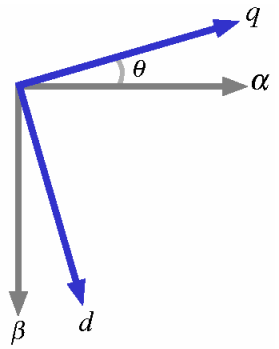

Figure 2 – Reference frames used in the transformations.

$$\begin{bmatrix} V_q \\ V_d \end{bmatrix} == \begin{bmatrix} \cos\theta & -sin\theta \\ sin\theta & \cos\theta \end{bmatrix} \begin{bmatrix} V_\alpha \\ V_\beta \end{bmatrix} \quad (1)$$

$$\begin{bmatrix} V_\alpha \\ V_\beta \end{bmatrix} = \begin{bmatrix} \cos\theta & sin\theta \\ -sin\theta & \cos\theta \end{bmatrix} \begin{bmatrix} V_q \\ V_d \end{bmatrix} \quad (2)$$

Hilbert Transformer-Based PLL

In [3] is presented a SRF PLL algorithm for single-phase systems, where the quadrature signal is generated through the use of the Hilbert transformer, as illustrated in Figure 3. For a real signal $x(t)$, the Hilbert transform (H) is defined as shown in eq. (3), where P is Cauchy principal value [6].

$$\hat{x}(t) = H(x) = \frac{P}{\pi}\int_{-\infty}^{\infty} \frac{x(\tau)}{t-\tau} d\tau \quad (3)$$

By using the Hilbert transformer, it is possible to generate a signal, which is orthogonal with the input signal. A Park transformation is then applied to generate the d and q-axis voltages, used in the control loop, in a way similar to the previous algorithm.

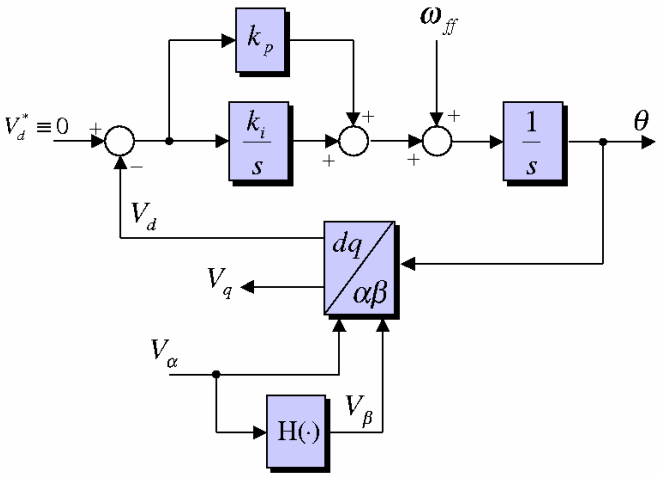

Figure 3 – Single-phase PLL algorithm based on a Hilbert transformer for the generation of the quadrature signal.

Transport Delay-Based PLL

Figure 4 shows a block diagram representation of a SRF PLL, based on the use of a transport delay to generate the quadrature signal. The delay is adjusted in order to give a *90* degrees phase-shift with respect to the fundamental frequency of the input signal. The basic difference of this method, compared with the Hilbert transformer method is that, in this case, all the harmonic content of the input signal is subjected to the same time delay. For the Hilbert transformer method, all the harmonic content is phase-shifted *90* degrees.

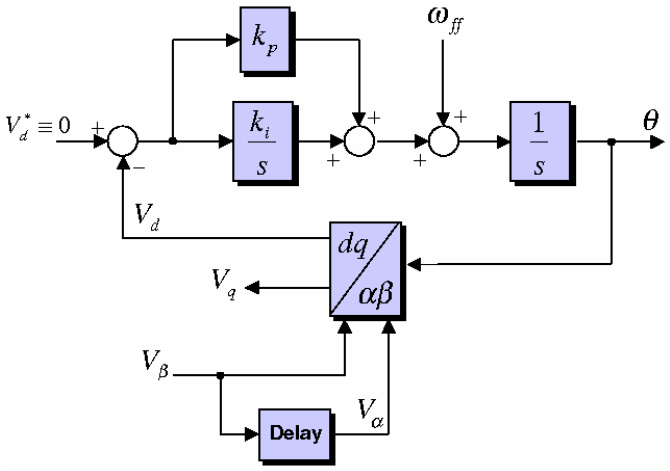

Figure 4 – Single-phase PLL algorithm based on the use of a transport delay to generate the quadrature signal.

III. Implementation Issues

Inverse Park-Based PLL

Although the algorithm of the PLL based on the inverse Park transformation is easily implemented, requiring only an inverse Park and two first-order low-pass filters, the tuning of its PI controller and the choice of the time constant of the filters is a more difficult process, as compared with the other PLL algorithms. This is due to the presence of the two interdependent nonlinear loops, which makes linearization and use of linear system analysis tools more troublesome processes.

Hilbert Transformer-Based PLL

Once the ideal Hilbert transformer, as defined in eq. (3) leads to a noncausal system, it is not practically realizable. However, it is possible to approximate the transformation through the use of a Finite Impulse Response (FIR) filter, with coefficients defined as [6]:

$$h[n] = \begin{cases} \dfrac{1-\cos[(n-0.5N)\pi]}{\pi(n-0.5N)} & \text{for} \quad n \neq 0.5N \\ 0 & \text{for} \quad n = 0.5N \end{cases} \quad (4)$$

where N is the filter order, n is the coefficient index ($0 < n < N$) and $h[n]$ are the coefficients of the filter. In eq. (4), if N is an odd number, the filter is high-pass and, if N is an even number, the filter is band-pass.

Figure 5 shows a block diagram representation of the FIR filter, where index q is defined in eq. (5). As it is seen, this implementation of the Hilbert transformer requires an input signal delayed by q samples, in order to generate output signals V_α and V_β with a phase displacement equal to $\pi/2$ for every frequency of interest. In Figure 5, the input signal is the grid voltage and the output signals are used as inputs for the Park transformation block in the *Hilbert transformer-based* PLL.

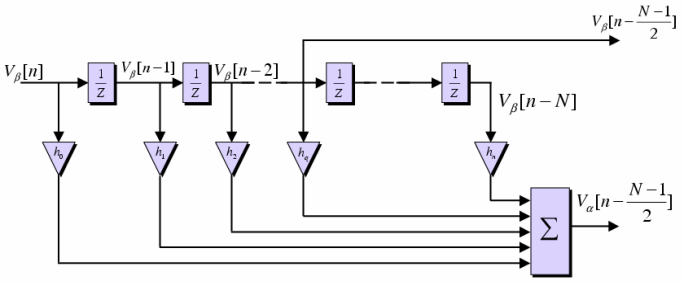

Figure 5 – Block diagram representation of the FIR filter.

$$q = \frac{N-1}{2} \tag{5}$$

Figure 6 shows the frequency response of the FIR filter for different orders, with a sampling frequency equal to *10kHz*. It is possible to see that for low order filters, the gain is strongly dependent on the frequency. This is particularly important for low frequency systems as utility applications, where it is possible to have a gain for the fundamental frequency lower than the gain for the harmonic components. As the filter order is increased, the gain approximates the unit for all frequencies. Table 1 shows the impact of the filter order over the output signal at the fundamental frequency.

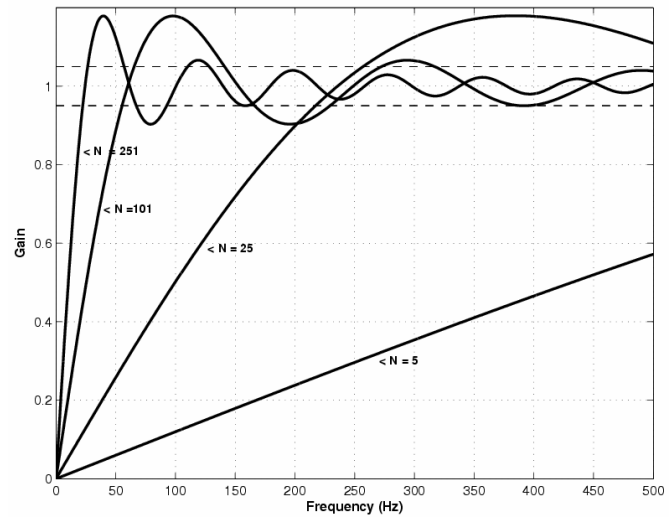

Figure 6 – Frequency response of the FIR filter for different orders. Sampling frequency equal to *10kHz*.

Table 1 - FIR filter response at *60H*. Sampling frequency *10kHz*.

Filter Order	Delay [ms]	Phase delay @ 60Hz [degrees]	Gain @ 60Hz
5	0.2	4.32	0.07
25	1.2	25.9	0.31
101	5.0	108.0	0.99
251	12.5	279.0	1.02

Analyzing Figure 6 and Table 1 it can be pointed out:

- For low order filters, the gain at the fundamental frequency is low, compared with the gains at harmonic frequencies, suggesting a PLL output highly affected by distortions in the input signal;
- For higher order filters, the added time delay makes the utilization of this algorithm not viable for on-line applications. In cases where the time delay is not a issue, the use of filters with higher orders can be an adequate solution for a more precise track of the phase angle of the input signal.

Transport Delay-Based PLL

The transport delay block is easily implemented through the use of a first-in-first-out (FIFO) buffer, with size set to one-fourth the number of samples contained in one cycle of the fundamental frequency. Generally speaking, the algorithm is easily implemented and the tuning process does not pose especial difficulties.

IV. Simulation Results

A simulation study was conducted to allow an evaluation of the operation of the PLL structures, especially under distorted utility conditions. The total harmonic distortion was purposely selected high (*THD > 10*), in order to allow a better visualization of the behavior of each algorithm. The PI controllers of each PLL were adjusted with the same gains. The Hilbert transformer was implemented with a FIR filter with order 5. The magnitude error for the fundamental components was corrected in the output of the filter.

Figure 7 shows the phase difference between the instantaneous angle of the fundamental component of the input signal and the output angle of each PLL. A voltage sag with residual voltage equal to *70%* and a phase angle jump of *30 degrees* was applied to each PLL input. All three PLLs have a very similar behavior in terms of settling time, what is explained by the fact that the gains of the PI controllers where set equally. However, the *inverse Park-based* PLL exhibits an output signal less affected by the presence of harmonics. In this case, the algorithm based on the Hilbert transformer presents an output more sensitive to harmonic distortions in the input signal.

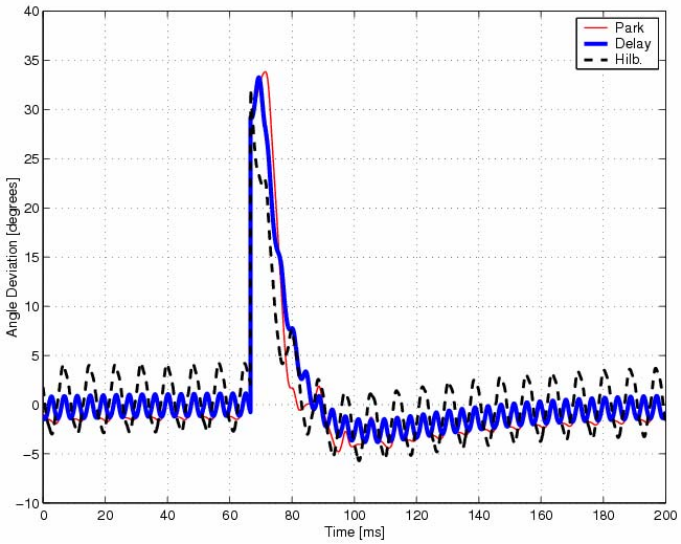

Figure 7 – Angle deviation during a voltage sag with *30 degrees* of phase-angle jump and residual voltage equal to *70%.*

Figure 8 shows the difference between the instantaneous amplitude of the fundamental component of the input signal and the amplitude information from each PLL. As in the previous case, a voltage sag with residual voltage equal to *70%* and a phase angle jump of *30 degrees* was applied to each PLL input. Although the amplitude deviation present a mean value close to zero for all PLLs, the *Hilbert Transformer-based* PLL exhibits an output very affected by the presence of harmonics. The steady-state peak-to-peak variation of the deviation present by the *transport delay-based* PLL and the *inverse Park-based* PLL are of the same magnitude.

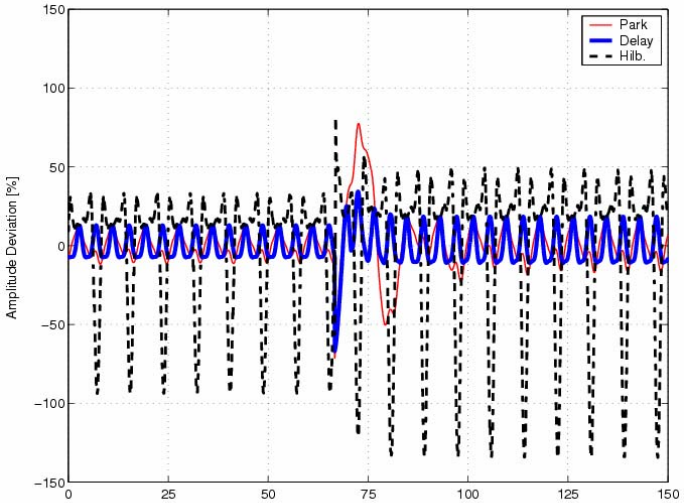

Figure 8 – Amplitude deviation during a voltage sag with *30 degrees* of phase-angle jump and residual voltage equal to *70%.*

V. EXPERIMENTAL RESULTS

The three PLL algorithms presented were implemented in a digital signal processor (DSP), suited for motion control and power electronics applications (*TMS320LF2407, Texas Instruments*). A clock frequency equal to *40MHz* and a sampling frequency equal to *10kHz* were used. The gains of the PLLs were all set with the same values.

Table 2 shows the processing time for each PLL, with the *Hilbert transformer-based* algorithm used as a reference. As it is seen, the *transport delay-based* PLL exhibits the lowest processing time, followed by the *inverse Park* algorithm.

Table 2 – Processing time for each PLL algorithm.

Algorithm	Processing Time
Inverse Park	86,4%
Hilbert Transformer	100%
Transport Delay	74,4%

Figure 9 to Figure 11 show the experimental results obtained for the PLL algorithms. As in the simulation study, an input signal with a high total harmonic distortion was purposely used to allow a better visualization of the PLLs behaviors with distorted conditions. In each figure, *Ch.1* is the instantaneous angle of the input signal; *Ch.2* is the angle of the fundamental component of the input signal; *Ch.3* is the output of the PLL; and *Ch.4* is the angle difference, between the output of the PLL and the angle of the fundamental component of the input signal (*Ch.4=Ch.3-Ch.2*).

As it can be seen, in terms of phase angle, all three PLL algorithms present very similar steady-state performances when subjected to distorted input conditions. Depending on the information required and on the level of harmonic content expected, a more adequate tuning for the PI controllers can be used.

Although the implementation of the Hilbert transformer through a FIR filter leads to a phase delay, as explained before, the knowledge of this delay allows it compensation to minimize the output error.

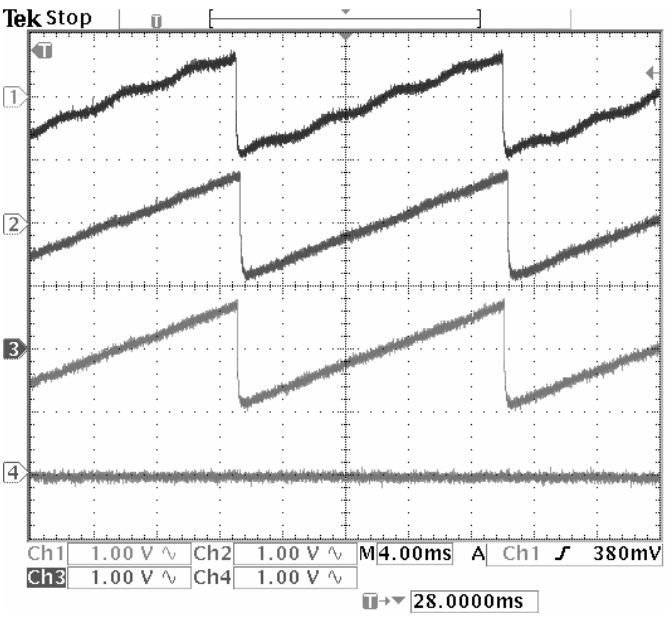

Figure 9 – *Inverse Park-based* PLL: instantaneous input angle (*Ch.1*); angle of the fundamental component of the input signal (*Ch.2*); angle generated by the PLL (*Ch.3*) and angle deviation (*Ch.4=Ch.3-Ch.2*).

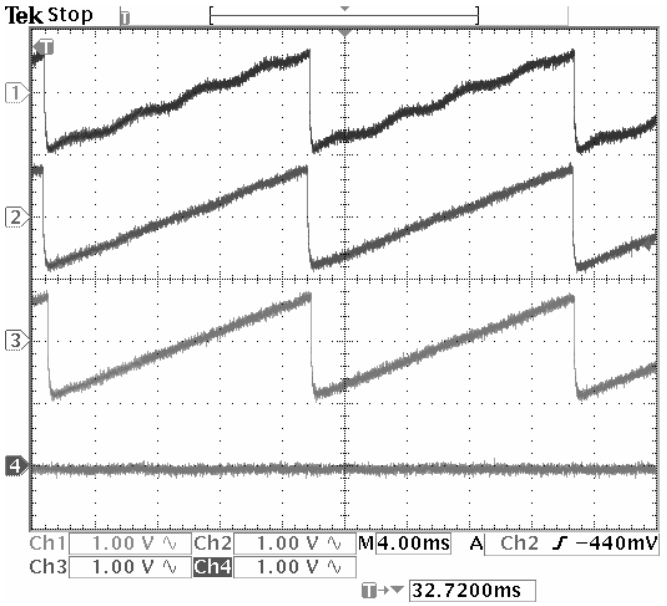

Figure 10 – *Hilbert transformer-based* PLL: instantaneous input angle (*Ch.1*); angle of the fundamental component of the input signal (*Ch.2*); angle generated by the PLL (*Ch.3*) and angle deviation (*Ch.4=Ch.3-Ch.2*).

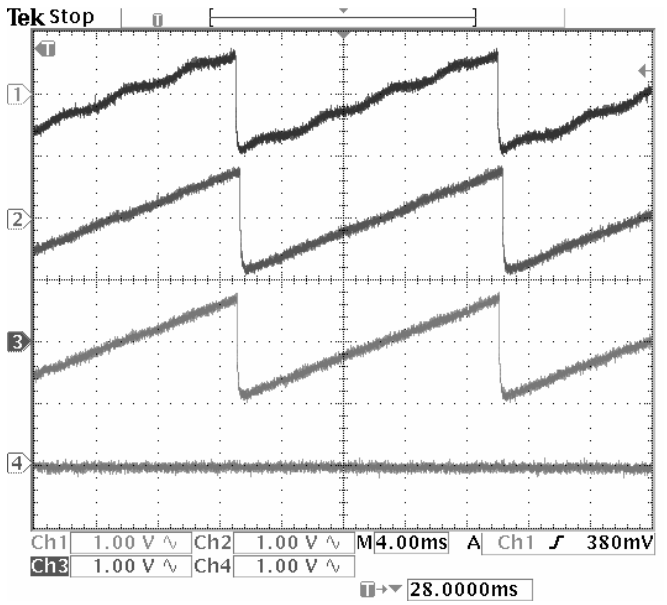

Figure 11 – *Transport delay-based* PLL: instantaneous input angle (*Ch.1*); angle of the fundamental component of the input signal (*Ch.2*); angle generated by the PLL (*Ch.3*) and angle deviation (*Ch.4=Ch.3-Ch.2*).

In addition to the evaluation of the operation of the PLL under distorted conditions, the algorithms were also evaluated with variations in the frequency of the input signal. For variations in the range expected for utility applications (*<1Hz*), no important deteriorations were observed in the operations of the PLLs.

VI. CONCLUSIONS

This paper presents a comparative study on PLL algorithms for single-phase utility connected applications. The algorithms considered are based on the use of a synchronous reference frame (SRF) to obtain information on amplitude, frequency and phase angle of a single-phase signal. The quadrature signal, required by the SRF algorithm, is generated with different strategies, depending on the PLL structure considered. It is shown that all algorithms allow the extraction of the required information from the input signal, even for input signals with high harmonic content.

In terms of load to the processing unit, the *Hilbert transformer-based* PLL present the worst behavior and the *transport delay-based* PLL represents a *25%* improvement in the performance. For the same set of PI controller gains, the angle and amplitude deviation encountered for the *inverse Park-based* PLL and the *transport delay-based* PLL have the same magnitude, in case of distorted input conditions. The *Hilbert transformer-based* PLL, implemented with a FIR filter of order 5 presents the worst general performance.

VII. REREFENCES

[1] – SILVA, Sidelmo M., ARRUDA, Lícia N. and CARDOSO FILHO, Braz de J. "Wide Bandwidth Single and Three-Phase PLL Structures for Utility Connected Systems". 9th. European Conference on Power Electronics and Applications. EPE2001. Graz, Austria. August, 2001.

[2] – ARRUDA, Lícia N., SILVA, Sidelmo M. and CARDOSO FILHO, "PLL Structures for Utility Connected Systems". 36th. Industry Applications Society Annual Meeting. IAS2001. Chicago, USA, 2001.

[3] – SAITOU, Nakoto, MATSUI, Mobuyuki and SHIMIZU, Toshihisa. "A Control Strategy of Single-phase Active Filter using a Novel d-q Transformation". 38th Industry Applications Society Annual Meeting. IAS2003. Salt Lake City, USA, 2003.

[4] – V. Kaura, and V. Blasko, "Operation of a phase locked loop system under distorted utility conditions," *IEEE trans. on Industry Applications*, vol. 33, no. 1, pp. 58-63, 1997.

[5] – G. Hsieh, and J.C. Hung, "Phase-locked loop techniques – a survey," *IEEE Trans. on Industrial Electronics*, vol. 43, no. 6, pp. 609-615, 1996.

[6] – MITRA, Sanjit K. Digital Signal Processing – A Computer-based Approach. McGraw-Hill International Editions, pp. 5-8. New York, USA, 1998.